Ag-zeolites as bactericidal additives in polymeric materials

J. L. Cerrillo, A. E. Palomares and F. Rey*

Instituto de Tecnología Química (Universitat Politècnica de València-Consejo Superior de Investigaciones Científicas, UPV-CSIC), Avenida de los Naranjos s/n, 46022 Valencia, Spain

* Corresponding author:
Fernando Rey
E-mail address: frey@itq.upv.es
Instituto de Tecnología Química, UPV-CSIC,
Camino de Vera s.n.,46022 Valencia (Spain)
(+34) 96 387 79686

ABSTRACT

In this work, different Ag-zeolites have been evaluated as biocide materials against two common bacteria, displaying an excellent bactericidal activity in different media. The results demonstrate that the amount of silver, the type of zeolitic structure and the zeolite Si/Al ratio strongly influence on their bactericidal activity. The higher Ag amount, the better antimicrobial activity; the larger pore opening of the zeolite and the closer to 2 Si/Al ratio, the better bactericidal effect. The characterization of Ag-zeolites by different techniques shows that the incorporation of Ag at the zeolites does not alter the zeolite structure and that Ag is incorporated as Ag^+ cations.

The most promising Ag-zeolites with a Si/Al ratio of 2 were introduced in a polymer matrix of polypropylene, showing very high biocide activity against *S.aureus*. The applicability of the resulting Ag-zeolite-polymer material is limited because its darkening due to the presence of reduced silver species. The incorporation of a photo-stabilizer does not decrease the biocide activity, while maintains the original color of the polypropylene polymer. It has been shown that lixiviated Ag^+ cations are the biocide active species. These Ag-species are released even when the Ag-zeolite is incorporated into the polymer, providing bactericide effects to the final Ag-zeolite-polymer composite.

KEYWORDS

Silver, zeolites, biocide, polymer, additive

1. INTRODUCTION

Biocide materials can be defined as materials with one or more active compounds intended to control, remove or destroy any organism by chemical or biological processes [1]. Biocides, and specifically antimicrobials, control the growth of bacteria, fungi, viruses and other microbials [2]. Although some of these microbials are necessary for our survival, others are infectious agents and can produce important problems both in human health and ecosystems [3].

Focus on medical environments [4-6], it is really important to preserve all the surfaces free of pathogenic microorganisms, responsible of most of Healthcare-Associated Infections (HAIs). Only at European intensive care units, 8.3% of the patients suffer these infections, causing 37000 death per year [7, 8]. An option to overcome this problem is to attach or to cover the surface of medical devices or furnishings with biocide materials, permitting the leaching of biocide substances into the surrounding environments [9]. However, these applications present several drawbacks, being the most important, their short-time effectiveness.

These medical applications must comply with the strict legal measures for being safe and the biocide materials must be sustainable and cost-effective [3]. The incorporation of biocide properties to diverse materials, such as polymers, paints, fibbers or glass is far from being trivial. Despite of legal requirements, the biocide materials must be resistant to autoclaving temperature, radiation and/or mechanic stress [10] and must possess a long-life biocide effectivity. A successful example is the incorporation of biocide substance in polymeric materials in order to inhibit the growth of

microorganisms, through the gradual release of the biocidal agent to the materials surface [11].

Among the different chemical substances with antimicrobial properties, inorganic materials present important advantages over organic agents. Indeed, inorganic biocides typically have a better chemical and thermal stability, mechanic resistance, safeness and longer biocide effects than organic ones [3]. One of the most recognized and used biocide is silver [10, 12]. This metal presents a broad antimicrobial spectrum, being active against diverse bacteria, fungi, viruses, yeast, and algae [13-15]. The biocide effects of silver are evident and 0.001 ppm of Ag^+ cations are effective in controlling bacteria populations, but at the same time, they present low toxicity for eukaryotic cells [16, 17]. It has been evidenced the multiple attack of Ag species on different bacteria organelles [18, 19], but the biocide mechanism of Ag^+ cations is not yet fully understood [20].

The incorporation of silver on carrier materials is a strategy to improve the gradual release of silver and to improve the biocide effect during time. Among all possible materials to support silver species, zeolites are one of the best choices [3, 21-23]. These aluminosilicates are inorganic, microporous, three dimensional and crystalline solids materials widely used in catalytic, separation and adsorption processes [24]. Zeolites present cation exchange capacity, permitting to incorporate cations inside zeolitic porous and channels and controlling their release [25]. Ag-zeolites have been studied as supported biocide substances by different authors at *in vitro* experiments against bacteria, virus and fungi [3, 10, 18, 26-31] and most of these studies showed a correlation between the biocide effects and the lixiviation of Ag [32]. However, for practical uses, the Ag-containing zeolite must be incorporated in final devices. The

studies of Ag-zeolites additives in polymers, surfaces, etc. are scarce. To our knowledge, most of them consist of Ag-zeolites in acrylic paints [27, 33] and some polymers [34-37].

Herein, we report the synthesis of diverse Ag-zeolites studying the influence of silver loading and zeolitic structure on the biocide activity. The Ag-zeolites were characterized by different physic-chemical techniques and their bactericidal properties were evaluated by *in vitro* tests against two common bacteria, *Staphylococcus aureus* and *Escherichia coli*. Afterwards, the most active biocide materials were embedded into a polypropylene matrix, preparing different multifunctional polymeric plates and their corresponding *in vivo* biocide activities were evaluated. Moreover, the photostability of the resulting active polymers has been improved by adding appropriated stabilizers to the final polymer blending. Finally, release experiments were carried out to evaluate the migration of the biocide species from the support or from the polymeric matrix to the external medium.

2. EXPERIMENTAL

2.1. Preparation of Ag-zeolites

Two types of zeolites with different Si/Al ratio were used: Linde Type A (LTA) and Faujasite (FAU). LTA with a Si/Al ratio of 1 (LTA-1) was supplied by Sigma-Aldrich (4A). LTA with a Si/Al ratio of 2 (LTA-2) was prepared using a gel composition of *1,19Na_2O:4,64TMAOH:Al_2O_3:6SiO_2:200H_2O* and LTA with a Si/Al ratio of 5 (LTA-5) was prepared with a gel composition of *19,7SiO_2:Al_2O_3:6TEAOH:4DEDMAOH:TMACl:NaCl:342H_2O* [38, 39]. FAU with Si/Al ratios of 1.3 and 2.4 were supplied by Zeolyst. The silver was incorporated to the zeolites by an ion-exchange procedure [22]. Samples were labelled as LTAAg or FAUAg depending the zeolitic structure, followed by the Si/Al ratio and by the ion-exchange percentage. Thus, LTAAg-1_50% is the zeolite with LTA structure with a Si/Al ratio of 1 and 50 % of Ag ion-exchange. When the percentage of silver is not indicated in the sample labelling, the amount of silver is 2 wt.%. Thus, sample FAUAg-2.4 is the zeolite with FAU structure with a Si/Al ratio of 2.4 and a 2 wt.% of Ag. The studied samples are shown in **Table 1**.

2.2. Characterization

A Varian 715-ES inductively coupled plasma-optical emission spectrometer (ICP-OES) was used to evaluate the chemical composition of the solids. For carrying out these experiments, 30 mg of each sample were digested for 24 h in an acid aqueous solution (10 vol.% HNO_3 and 3.3 vol.% HF). On the other hand, the concentration of

silver in liquid samples was analyzed using an atomic absorption spectrometer with a Zeeman graphitic furnace, Varian SpectrAA 240Z-GTA120.

X-ray diffraction analysis was carried out using a X'pert Panalytical diffractometer with monochromatic CuK$\alpha_{1,2}$ radiation (λ = 1.5406, 1.5444 Å; Kα_2/Kα_1 intensity ratio = 0.5). Crystallinity and purity of modified-zeolites were checked and identified using the JCPDS files.

Hydrogen temperature programmed reduction (H_2-TPR) was carried out with a TPD-TPR Autochem 2910 equipment with a thermal conductivity detector (TCD). Approximately 100 mg of each sample was loaded in a quartz cell and treated under Ar flow during 30 min. Subsequently, the gas flow was changed to a mix H_2:Ar (1:9) and the temperature was increased from room temperature up to 750 °C with a ramp of 10 °C/min.

Field Emission Scanning Electronic Microscope (FESEM) equipped with an energy dispersive X-ray spectroscopic device (EDS) was used to evaluate the morphology of the samples and to determine the composition and distribution of the elements in the samples. The measures were performed with a ZEISS ULTRA 55 equipment working at 20 keV.

2.3. Polymeric plates preparation

Polypropylene SABIC 71KE71PS was combined with Ag-zeolites and, in some cases, also with commercial HALS additive (hindered amine light stabilizer) creating the polymeric plates. The preparation of the functionalized polypropylene was made employing an internal intensive load mixer. This procedure permitted the adequate incorporation of the additives to the polymer with a homogenous distribution. The

polymeric plates were prepared using 40 g of mixed material that was introduced during 5 min in the mixer at 180 °C. Once the mixture was ready, the blending was transferred to a hydraulic press with temperature regulation where squared plates with 2.1 mm depth were prepared during 2 min at 200 °C. Finally, the square plates were immersed in cold water (quenching) for 1 min obtaining a flat plate.

2.4. Antimicrobials tests

Bactericidal experiments were performed with two different bacteria: *Staphilococcus aureus* CECT 240, one of the most usual Gram-positive bacteria and *Escherichia coli* CECT 516, one of the most common Gram-negative bacteria. The *in vitro* experiments were performed according to the macro-dilution method describe by Clinical and Laboratory Standards Institute [40]. This method evaluates the minimum inhibitory concentration (MIC), meaning, the lowest concentration of the biocide material that inhibits the bacterial growth [41]. Different Ag-zeolite solutions (1, 0.1, 0.3, 0.03, 0.003 and 0 wt.%) were prepared using tryptic soy broth (TSB) or peptone water (PW) as solvent. The solutions were inoculated with the bacterium, in the mid-exponential phase of growth, obtaining a final concentration of $1x10^5$ CFU/ml and then, incubated at 37 °C for 24 h. After this incubation time, serial decimal dilutions were prepared and 1 ml of these solutions was sub-cultivated on Plate Count Agar plates (PCA: peptone, yeast extract, glucose and agar). After a second incubation time at same conditions, colony forming units (CFUs) were evaluated, obtaining the MIC value for each sample by comparison with the control sample (blank) [42].

The determination of the bactericidal effect by *in vivo* experiments was evaluated over polymeric plates, following JIS Z 2801:2010 standard (ISO 22196:2007). This standard evaluates specifically the antimicrobial effectivity of no-porous materials, as polypropylene. 400 mL of *S.aureus* suspension ($2.5x10^5$ to $10x10^5$ cell/mL), prepared

using nutritive broth, was deposited over the polymeric plate and a very thin polyethylene blade was placed over the suspension to force the contact between the bacterial medium and the polypropylene plate. After 24 h of incubation at 37 °C with a relative humidity higher than 90 %, the liquid suspension was recovered with a syringe and decimals dilutions were performed with subsequent sub-cultivation at PCA plates. Finally, after 24 h of incubation of the PCA plates, the CFUs were counted at each PCA plate. The bactericidal effect of each Ag-zeolite/polymer was evaluated using the R value (

Equation 1) or the percentage of reduction of bacteria population (compared with the blank). R values equal or higher than 2 are related with positive bactericidal effects and those materials could be considered as bactericidal materials.

Equation 1: Calculation of the biocidal parameter R (Standard JIS Z 2108-2010)

$$R = log\left(\frac{\frac{CFUs}{mL} of\ control\ sample}{\frac{CFUs}{mL} of\ problem\ sample}\right)$$

2.5. Lixiviation studies

The amount of Ag released from the zeolites was determined according to Liu et al. [43]. The lixiviation of Ag from the zeolites was studied with suspensions of 100 ppm of Ag-zeolites in PW. During one day, different aliquots of the suspensions were extracted and analyzed by GFAAS to evaluate the amount of Ag released from the zeolite to the biological broth. On the other hand, the Ag lixiviated from the functionalized polymeric plates was measured following the standard JIS Z 2108:2010 without the incorporation of the bacteria in the medium. After the incubation and sub-cultivation periods, liquid samples were taken and the Ag concentration was analyzed by GFAAS.

3. RESULTS & DISCUSSION

3.1. Characterization results

Figure 1 displays the X-Ray patterns of the Ag-exchanged LTA-2 zeolites (green patterns) showing the characteristic peaks of LTA zeolites [45, 46] at 2θ = 7.22°, 10.21°, 12.50°, 21.71°, 24.04°, 27.16°, 29.99° and 34.42° (JCPDS: 00-38-0241), indicating that the incorporation of silver to the zeolite does not modify the zeolitic structure [22]. However, depending on the amount of silver in each zeolite, the XRD peaks have different intensities. This modification can be explained by the diverse scattering factor of Ag and Na. Besides, no any diffraction peak assigned to silver oxide or metallic silver [3, 44] is observed. This strongly suggest that cationic silver (Ag^+) are the main silver species within the Ag-exchanged zeolites. Similar results were obtained with the Ag-LTA with different Si/Al ratios and with the Ag-FAU.

Chemical composition of as-prepared Ag-zeolites and parent zeolites are listed in **Table 1**. The Ag content obtained by ICP-OES (bulk technique) and EDS (punctual technique) is very similar, demonstrating that silver is homogeneously distributed in the zeolite. Besides, comparing the samples with a theoretical exchange degree of 100%, it can be seen that FAU-type materials and LTA-1 almost get theoretical exchange values; meanwhile LTAs with Si/Al ratio of 2 and 5 do not get the expected total exchange.

As can be seen at **Figure 2**, the incorporation of high amount of Ag in FAU-2.4 does not modify the morphology and size of the zeolitic crystals. These evidences had been already observed with Ag-LTA in previous studies [18, 22], indicating that the incorporation of Ag in the zeolitic materials does not modify the structure, as XRD results have already shown.

H_2-TPR studies of almost total exchanged LTA zeolites with different Si/Al ratio (**Figure 3**) have been performed. Although, the three samples have Ag^+ as initial Ag species [22], the three profiles are different. This is probably due to the different amount of silver and to the different distribution and location of the Ag^+ species inside the zeolite. In the case of LTAAg-2_100% and LTAAg-5_100%, the first positive peak appears between 100-125 °C whilst it appears close to 150ºC for the LTAAg-1_100%. This peak can be related to the reduction of Ag^+ at different positions of the zeolitic structure producing Ag_m^{n+} clusters or metallic Ag [47]. However, since no further hydrogen consumption is observed in the TPR experiments, total reduction of the Ag^+ to Ag^0 is assumed. Moreover, the most significative observation in the TPR profiles of the two LTA samples with higher Si/Al ratio is the presence of negative signals, corresponding to H_2 release. In the case of LTAAg-2_100%, the negative signal appears at 420 °C with a shoulder at 450 °C, and in the case of LTAAg-5_100% the negative peak appears at 325 and 420 °C. The released H_2 can be attributed to the re-oxidation of Ag^0 by protons at relatively high temperature, as it has been previously reported by Berndt et al. [48]. The results indicate that the Ag amount and the Si/Al ratio influence in the reducibility of Ag species, and this can be related with their different location in the zeolitic framework and then, with their mobility, as it has previously reported by Ferreira et al. [3] based on XPS data analyses.

3.2. *In vitro* bactericidal results

The bactericidal effects of the LTAAg-1_100% was evaluated against both *S.aureus* and *E.coli* bacteria in two different media (TSB and PW) by *in vitro* tests. As **Figure 4** shows, the lowest values of MIC were obtained in PW media against both bacteria. This

can be explained due to the different type of broth media, PW is less nutritive than TSB. Thus, bacteria exhibit less resistant in PW than in TSB broth. To a better study of the biocide effects, henceforth, experiments were carried out at TSB broth permitting to see differences in the biocide activity of the studied Ag-zeolites.

The biocide activity of fully Ag-exchanged LTA zeolites having different Si/Al ratios are shown in **Figure 5 (left)**. There, it is observed that the lowest MIC for both bacteria is provided by the zeolite presenting Si/Al ratio close to 2. Similar results were obtained for 50% Ag^+ exchanged LTA zeolites **Figure 5 (right)**, suggesting that the bactericide effect relays more in the Si/Al ratio of the carrier than on the metal loading. Indeed, the best MIC value was obtained for the LTAAg-2-50% sample, even presenting lower Ag content.

Similar results were obtained with total exchanged FAU zeolites with different Si/Al ratio, being more active the FAUAg-2.4_100% than FAUAg-1.3_100%, even with less amount of Ag at its composition. These results indicate that the Si/Al ratio of 2 is the optimum to obtain the best bactericide effects, independently the zeolitic structure.

On the other hand, three total exchanged Ag-LTA were calcined during 10 h at 550 °C and their bactericidal activity was also studied. This thermic treatment does not result in any improvement in the biocide activity, even a decrease on this effect is shown for the three zeolites against both bacteria. These results indicate that the silver species obtained during the thermic treatment are less active against bacteria than as prepared Ag-zeolites.

We followed our study decreasing the silver content of the zeolite down to 2 wt.% for accomplishing with legal limitations and to have less silver content than in commercial Ag-zeolites with biocide applications such as Agion® or Zeomic® [49-51].

The outcomes reported in **Figure 6** show that these zeolites still present important biocidal capacity, but as expected, lower than the fully and half exchanged zeolites, demonstrating the influence of the amount of Ag in the biocide activity. Low Ag content zeolites having large pores (FAU) show lower MIC values and then, better biocide activities. The larger pore opening and the presence of supercavities of FAUs (7.4x7.4 Å), in comparison with LTAs (4.1x4.1 Å), favor the release of Ag^+ cations to the media, increasing their bactericidal activities [52, 53]. Finally, comparing the same structures with different Si/Al ratio and similar Ag content, in both LTA and FAU zeolites, the best bactericide activity was observed on zeolites with a Si/Al ratio close to 2.

Furthermore, all bactericidal experiments present much higher MIC values for S.*aureus* than for *E.coli*. The lower biocidal activity of Ag-zeolites against *S.aureus* could be attributed to the wider peptidoglycan layer of Gram-positive cells compared with Gram-negative bacteria, that results in a higher resistance to the Ag^+ [54].

3.3. Lixiviation studies

The different biocide activity obtained when changing Ag amount on the zeolite, Si/Al ratio of topology suggests that the biocide mechanism is related to the release of Ag^+ cations to the medium where bacteria are found [31].

Demirci et al. carried out lixiviation experiments with zeolites with high Ag content [55]. The authors describe high lixiviation at the very beginning and a gradually abatement. Others authors have studied the Ag release in biological media with bacteria obtaining higher release rates. In our case, we have performed release experiments to elucidate the Ag^+ release rate of selected Ag-zeolites presenting different structures

(FAU and LTA) and diverse Si/Al ratios (LTA-1 and LTA-2). **Figure 7** shows the percentage of released Ag versus time of leaching, showing a progressive lixiviation of the bactericidal agent during the first 8 h and later reaching a plateau. After 24 h, FAUAg-2.4 releases 20% of total Ag to the media, while for LTAAg-2 and LTAAg-1 release 10% and 6%, respectively. Comparing the Ag release curves, it is clear that the lixiviation of the biocide agent strongly depends on the zeolitic structure and less importantly on the Si/Al ratio. The rates of Ag release of the different zeolites are in agreement with the biocidal activities, suggesting that the presence of Ag^+ in the media is the controlling parameter of biocide activity.

3.4. Biocidal polymers, *in vivo* tests

The polymeric plates were functionalized by incorporating different amounts (0.2, 0.4 and 1 wt.%) of Ag-containing zeolites with 2 wt.% of Ag and optimum Si/Al ratio of 2 (**Table 2**). The incorporation of different percentages of Ag-zeolites produced different level of darkness at the polymeric plates (**Figure 8)**, an undesirable effect for the application of the polymer as, for instance, covering material. The darkening of the polymer increases as the Ag-zeolite content does. This color modification does not come exclusively from the incorporation of Ag-zeolites, also, the reduction of Ag^+ to Ag^0 during the thermic treatment, need for the preparation of the functionalized polymeric material, is responsible for the darkening of the polymer [56]. Identical studies with parent zeolites (Na-zeolites) did not show any modification of the polymeric plates (images not shown), confirming that silver is the darkening substance.

To minimize this effect we only evaluated the bactericide effects of materials with 0.2 or 0.4 wt.% of Ag-zeolites. The results presented in **Figure 9** shows that the Ag-

zeolite functionalized polymers present a remarkable biocide activity, reaching even 100 % reduction against *S.aureus* at *in vivo* experiments for some of the essayed polymers. The biocidal activity of Ag-zeolite-polymer composites increases as the Ag content does, being more clearly observed at LTA, because the very high activity of FAU reaches nearly full reduction, even for the polymer that contains less Ag-FAU zeolite.

Nevertheless, still some darkening of the material remains and restricts its possible application. In order to improve it, a photochemical stabilizer so-called HALS (hindered amine light stabilizers coming from 2,2,6,6-tetrametylpipedinine) has been added. HALS are usually used to protect polymers from negative photo-effects of free radicals and others substances. We have prepared new polypropylene blends using HALS and Ag-zeolites, using the same method than before and evaluating their biocidal activity (**Table 2**). The visual inspection of the polymers indicates that HALS successfully prevents the darkness at polymeric plates. Moreover, incorporation of HALS does not decrease the biocidal effects of the Ag-zeolites, presenting almost total reduction of the CFU and even higher R values than the composites without HALS (**Table 2**). Thus, according to the standard, these materials can be defined as bactericidal materials. However, to confirm that the biocidal properties of optimum Ag-zeolite-HALS-polymer composite are due to the presence of Ag cations, a blank experiment has been carried out. A similar composite prepared skipping the presence of Ag-zeolite was essayed as biocidal material. This test showed neglectable R values and percentages of reduction lower than 20%, confirming that in absence of silver there is not biocidal activity.

3.5. Lixiviation studies

The release of Ag from functionalized polypropylene polymeric plates (following standard JIS Z 2108:2010 procedure without bacteria) is shown in **Figure 10**. The results indicate that the highest amount of Ag in the polymeric system, the highest release of Ag^+ to the media and, therefore the best bactericidal activity. Moreover, the incorporation of HALS favors the lixiviation of Ag^+, confirming that its presence in the polymeric matrix improves the biocidal activity, besides of keeping the visual aspect.

4. CONCLUSIONS

The Ag-zeolites show excellent bactericidal activity in different bacteria growth media against both *S.aureus* and *E.coli* bacteria. The results demonstrate that the amount of Ag, the type of zeolitic structure and the Si/Al ratio of the zeolite are the most important variables to obtain the best bactericidal activity. In that sense, best results were obtained with zeolites containing higher amount of silver and exhibiting largest pore opening and Si/Al ratio close to 2. Ag-zeolites were characterization by different techniques showing that the incorporation of Ag at zeolites does not modify the structure of the zeolite, being the main silver species the exchanged Ag^+ cation.

The real applicability of the most promising Ag-zeolites as biocide materials was studied through the functionalization of propylene with Ag-zeolites presenting Si/Al ratio of 2. The Ag-zeolite-polymer composite has a very high biocide activity against *S.aureus*. However, the incorporation of Ag-zeolites at the polymeric formulation is limited due to the darkening of the sample, probably because of the presence of reduced silver species. To solve this, a photo-stabilizer substance (HALS) was incorporated to

the new polymeric formulation. This new Ag-zeolite-HALS-polypropylene composites keeps the bactericide activity of the polymeric material and also maintains the color of the original polymer.

Finally, lixiviation studies were carried out with the Ag-zeolite and with the functionalized polymer composites. The results reveal that the release of Ag is related to the bactericidal effects and silver can even release from the Ag-zeolites that are embedded in the polymeric matrix.

ACKNOWLEDGEMENT

The authors thank the Spanish Ministerio de Economia y Competitividad and Fondo Europeo de Desarrollo Regional through RTI2018-101784-B-I00 (MINECO/FEDER) and SEV-2016-0683 for the financial support. J.L. Cerrillo wishes to thank MINECO for the Severo Ochoa PhD fellowship (SVP-2014-068600).

REFERENCES

[1] L. Ruiz, A. Alvarez-Ordóñez, The role of the food chain in the spread of antimicrobial resistance (AMR), R. Boukherroub, S. Szunerits, D. Drider (Eds.), Functionalized Nanomaterials for the Management of Microbial Infection, Elsevier, 2017, p. 23-47.

[2] N. Tucker, Clean production, Green Composites, 2017, p. 95-121.

[3] L. Ferreira, A.M. Fonseca, G. Botelho, C. Almeida-Aguiar, I.C. Neves, Microporous and Mesoporous Materials, 160 (2012) 126-132.

[4] I. Johansson, P. Somasundaran, Handbook for Cleaning/decontamination of Surfaces, Elsevier, 2007.

[5] C. Marambio-Jones, E.M. Hoek, Journal of Nanoparticle Research, 12 (2010) 1531-1551.

[6] W.K. Loke, S.K. Lau, L.L. Yong, E. Khor, C.K. Sum, Journal of Biomedical Materials Research: An Official Journal of The Society for Biomaterials, The Japanese Society for Biomaterials, and The Australian Society for Biomaterials and the Korean Society for Biomaterials, 53 (2000) 8-17.

[7] ECDPC, Annual Epidemiological Report 2015 European Centre for Disease Prevention and Control, 2017.

[8] Y.-L. Wu, X.-Y. Yang, X.-X. Ding, R.-J. Li, M.-S. Pan, X. Zhao, X.-Q. Hu, J.-J. Zhang, L.-Q. Yang, Journal of Hospital Infection, 101 (2019) 231-239.

[9] A. Jain, L.S. Duvvuri, S. Farah, N. Beyth, A.J. Domb, W. Khan, Advanced healthcare materials, 3 (2014) 1969-1985.

[10] Y. Inoue, M. Hoshino, H. Takahashi, T. Noguchi, T. Murata, Y. Kanzaki, H. Hamashima, M. Sasatsu, Journal of inorganic biochemistry, 92 (2002) 37-42.

[11] M. Turalija, S. Bischof, A. Budimir, S. Gaan, Composites Part B: Engineering, 102 (2016) 94-99.

[12] L. Ferreira, A.M. Fonseca, G. Botelho, C. Almeida-Aguiar, I.C. Neves, Microporous Mesoporous Mater., 160 (2012) 126-132.

[13] C. Anfray, B. Dong, S. Komaty, S. Mintova, S. Valable, ACS applied materials & interfaces, 9 (2017) 13849-13854.

[14] T. Haile, G. Nakhla, J. Zhu, H. Zhang, J. Shugg, Microporous and Mesoporous Materials, 127 (2009) 32-40.

[15] M. Khowdiary, A. El-Henawy, A. Shawky, M. Sameeh, N.A. Negm, Journal of Molecular Liquids, 230 (2017) 163-168.

[16] R. Giangiordano, D. Klein, Letters in applied microbiology, 18 (1994) 181-183.

[17] W. Ghandour, J.A. Hubbard, J. Deistung, M.N. Hughes, R.K. Poole, Applied microbiology and biotechnology, 28 (1988) 559-565.

[18] J.L. Cerrillo, A.E. Palomares, F. Rey, S. Valencia, M.B. Pérez-Gago, D. Villamón, L. Palou, ChemistrySelect, 3 (2018) 4676-4682.

[19] Q.L. Feng, J. Wu, G.Q. Chen, T.N. Kim, J.O. Kim, J. Biomed. Mater. Res., 52 (2000) 662-668.

[20] K. Mijnendonckx, N. Leys, J. Mahillon, S. Silver, R. Van Houdt, Biometals, 26 (2013) 609-621.

[21] P. Lalueza, M. Monzon, M. Arruebo, J. Santamaria, Mater. Res. Bull., 46 (2011) 2070-2076.

[22] J. Cerrillo, A. Palomares, F. Rey, S. Valencia, L. Palou, M.B. Pérez-Gago, Microporous and Mesoporous Materials, 254 (2017) 69-76.
[23] S. Malic, S. Rai, J. Redfern, J. Pritchett, C.M. Liauw, J. Verran, L. Tosheva, Colloids and Surfaces B: Biointerfaces, 173 (2019) 52-57.
[24] K. Na, M. Choi, R. Ryoo, Microporous and Mesoporous Materials, 166 (2013) 3-19.
[25] M. Yoldi, E. Fuentes-Ordoñez, S. Korili, A. Gil, Microporous and Mesoporous Materials, (2019).
[26] R. Guerra, E. Lima, M. Viniegra, A. Guzman, V. Lara, Microporous Mesoporous Mater., 147 (2011) 267-273.
[27] R.S. Bedi, R. Cai, C. O'Neill, D.E. Beving, S. Foster, S. Guthrie, W. Chen, Y. Yan, Microporous Mesoporous Mater., 151 (2012) 352-357.
[28] B. Kwakye-Awuah, C. Williams, M. Kenward, I. Radecka, Journal of Applied Microbiology, 104 (2008) 1516-1524.
[29] C. Chiericatti, J.C. Basílico, M.L.Z. Basílico, J.M. Zamaro, Microporous and Mesoporous Materials, 188 (2014) 118-125.
[30] P. Saint-Cricq, Y. Kamimura, K. Itabashi, A. Sugawara-Narutaki, A. Shimojima, T. Okubo, European Journal of Inorganic Chemistry, 2012 (2012) 3398-3402.
[31] J. Hrenovic, J. Milenkovic, I. Goic-Barisic, N. Rajic, Microporous and Mesoporous Materials, 169 (2013) 148-152.
[32] P. Lalueza, M. Monzon, M. Arruebo, J. Santamaria, Chem. Commun., 47 (2011) 680-682.
[33] Z. Iyigundogdu, S. Demirci, N. Bac, F. Şahin, Turkish Journal of Biology, 38 (2014) 420-427.
[34] M.M. Cowan, K.Z. Abshire, S.L. Houk, S.M. Evans, Journal of Industrial Microbiology and Biotechnology, 30 (2003) 102-106.
[35] H. Shi, F. Liu, L. Xue, Journal of membrane science, 437 (2013) 205-215.
[36] A. Fernández, E. Soriano, P. Hernández-Muñoz, R. Gavara, Journal of food science, 75 (2010) E186-E193.
[37] L.O. de Araújo, K. Anaya, S.B.C. Pergher, Coatings, 9 (2019) 786.
[38] US3375205A, R.L. Wadlinger, E.J. Rosinski, C.J. Plank, 1968, Mobil Oil Corp. . Synthetic zeolite catalyst for hydrocarbon conversion
[39] WO2003068679A1, J.G. Moscoso, G.J. Lewis, J.L. Gisselquist, M.A. Miller, L.M. Rohde, 2003, UOP L.L.C., USA . Crystalline aluminosilicate zeolitic composition: UZM-9
[40] A.L. Barry;, W.A. Craig;, H. Nadler;, L.B. Reller;, C.C. Sanders;, J.M. Swenson, Approved Guideline CLSI document, M26-A (1999).
[41] Y. Matsumura, K. Yoshikata, S.-i. Kunisaki, T. Tsuchido, Appl. Environ. Microbiol., 69 (2003) 4278-4281.
[42] K. Kawahara, K. Tsuruda, M. Morishita, M. Uchida, Dent. Mater., 16 (2000) 452-455.
[43] H. Liu, Q. Chen, L. Song, R. Ye, J. Lu, H. Li, J. Non-Cryst. Solids, 354 (2008) 1314-1317.
[44] A. Mayoral, T. Carey, P.A. Anderson, I. Diaz, Microporous Mesoporous Mater., 166 (2013) 117-122.
[45] V. Gramlich, W.M. Meier, Z. Kristallogr., Kristallgeometrie, Kristallphys., Kristallchem., 133 (1971) 134-149.
[46] A. Corma, F. Rey, J. Rius, M.J. Sabater, S. Valencia, Nature, 431 (2004) 287-290.

[47] D. Chen, Z.-P. Qu, S.-J. Shen, X.-Y. Li, Y. Shi, Y. Wang, Q. Fu, J.-J. Wu, Catal. Today, 175 (2011) 338-345.
[48] H. Berndt, M. Richter, T. Gerlach, M. Baerns, J. Chem. Soc., Faraday Trans., 94 (1998) 2043-2046.
[49] D.L. Boschetto, L. Lerin, R. Cansian, S.B.C. Pergher, M. Di Luccio, Chem. Eng. J., 204-206 (2012) 210-216.
[50] P. Lalueza, M. Monzón, M. Arruebo, J. Santamaria, Chemical Communications, 47 (2011) 680-682.
[51] M. Corrales, A. Fernández, J.H. Han, Antimicrobial packaging systems, Innovations in food packaging, Elsevier, 2014, p. 133-170.
[52] K.O. Kongshaug, H. Fjellvag, K. Petter Lillerud, Microporous Mesoporous Mater., 39 (2000) 341-350.
[53] W.H. Baur, Am. Mineral., 49 (1964) 697-704.
[54] L.M. Prescott, J.P. Harley, D.A. Klein, Microbiología, McGraw Hill - Interamericana de España, España, 2010.
[55] S. Demirci, Z. Ustaoglu, G.A. Yilmazer, F. Sahin, N. Bac, Appl. Biochem. Biotechnol., 172 (2014) 1652-1662.
[56] A.M. Pereyra, M.R. Gonzalez, V.G. Rosato, E.I. Basaldella, Prog. Org. Coat., 77 (2014) 213-218.

CAPTION FIGURES

Figure 1: XRD patterns of LTA-2 with different Ag content (greens) and of the parent LTA zeolites with different Si/Al ratio (Na form)

Figure 2: FESEM images of parent FAU-2.4 and

Figure 3: TPR profiles of the LTA zeolites completely exchange with Ag (LTAAg-1_100%; LTAAg-2_100%; LTAAg-5_100%)

Figure 4: Bactericidal activity (MIC) against *S.aureus* and *E.coli* in TSB and PW broth of LTAAg-1_100%.

Figure 5: Bactericidal activity (MIC) against *S.aureus* and *E.coli* in TSB with total and half silver exchange LTA zeolites.

Figure 6: Bactericidal activity (MIC) against *S.aureus* and *E.coli* in TSB with different zeolites with 2 wt.% Ag.

Figure 7: Ag lixiviation studies of three different zeolites at PW

Figure 8: Images of the polymeric plates prepared with different % and diverse Ag-zeolites

Figure 9: Biocidal properties of the surface of polymeric plates functionalized by different amount of LTAAg-2 and FAUAg-2.4, following JIS Z 2108:2010

Figure 10: Percentage of released Ag from different polymeric plate

TABLES

Table 1: Chemical composition of the zeolites measured by ICP-OES[a] and EDS[b]

Ag-zeolites	Wt.% Ag[a]	Ag Exchange (%) [a]	Si/Al molar ratio[a]	Wt.% Na[a]	Wt.% Ag[b]
LTA-1	-	-	1.0	15.3	-
LTAAg-1_100%	48.4	95.9	0.9	0.5	49.1
LTAAg-1_50%	29.0	50.1	0.9	7.9	-
LTAAg-1	1.8	2.7	0.9	13.9	1.9
LTA-2	-	-	2.0	9.7	-
LTAAg-2_100%	30.8	83.9	1.9	0.8	27.4
LTAAg-2_50%	17.2	38.6	2.1	-	-
LTAAg-2	2.2	6.0	1.9	6.1	6.1
LTA-5	-	-	4.9	5.6	-
LTAAg-5_100%	18.0	77.9	4.6	1.0	20.9
LTAAg-5_50%	8.3	43.0	5.0	-	-
LTAAg-5	1.9	8.7	4.8	5.1	1.5
FAU-1.3	-	-	1.3	13.9	-
FAUAg-1.3_100%	46.7	92.2	1.3	-	40.9
FAUAg-1.3	2.3	5.3	1.4	9.9	2.0
FAU-2.4	-	-	2.4	9.6	-
FAUAg-2.4_100%	30.6	93.4	2.5	1.2	32.5
FAUAg-2.4	1.3	3.5	2.4	6.8	1.6

Table 2: Composition of different polymer plates (%) and the bactericidal activity represented by R value

Ag-zeolites	Polypropylene (%)	Ag-zeolite (%)	HALS (%)	R
0.2% LTAAg-2	99.8	0.2	-	0.4
0.4% LTAAg-2	99.5	0.4	-	3.2
0.4% LTAAg-2 + HALS	99.2	0.4	0.4	3.7
0.2% FAUAg-2.4	99.7	0.2	-	1.7
0.4% FAUAg-2.4	99.4	0.4	-	3.3
0.4% FAUAg-2.4 + HALS	99.3	0.4	0.3	4.1

FIGURES

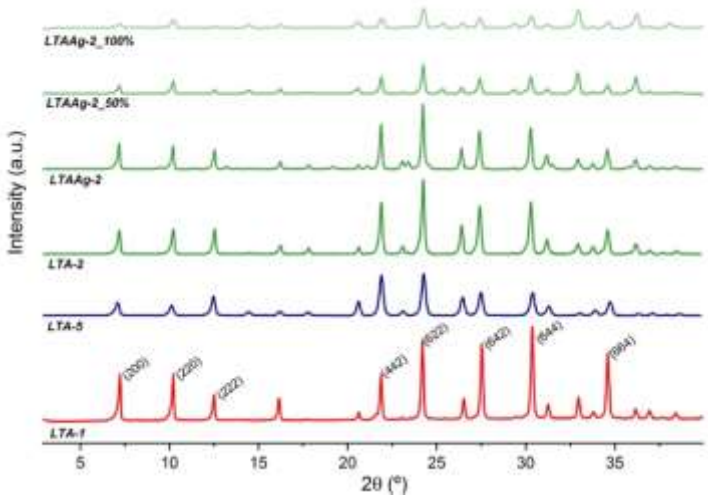

Figure 1: XRD patterns of LTA-2 with different Ag content (greens) and of the parent LTA zeolites with different Si/Al ratio (Na form)

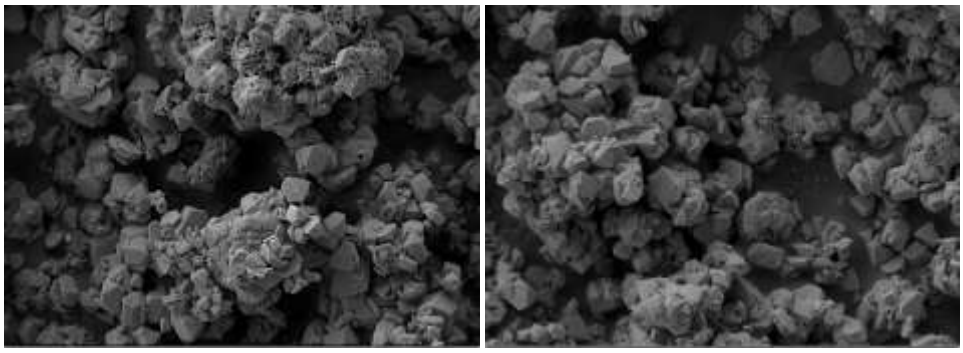

Figure 2: FESEM images of parent FAU-2.4 and FAUAg-2.4_100%.

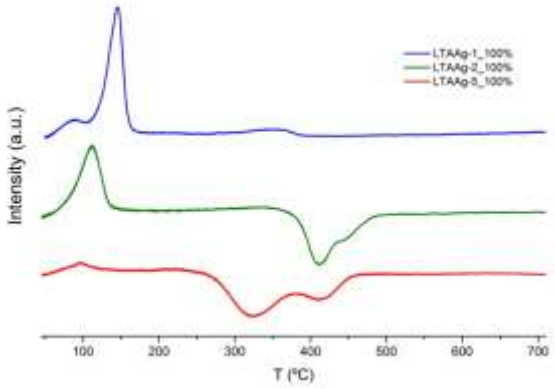

Figure 3: TPR profiles of the LTA zeolites completely exchange with Ag (LTAAg-1_100%; LTAAg-2_100%; LTAAg-5_100%)

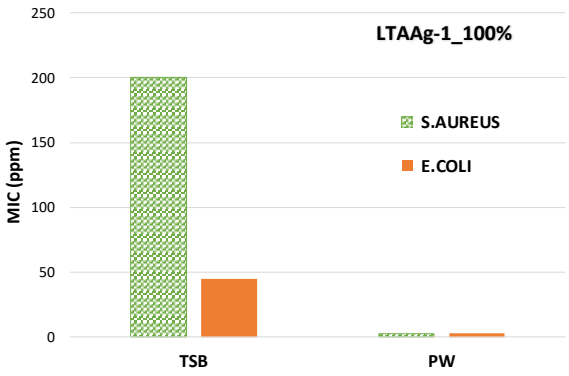

Figure 4: Bactericidal activity (MIC) against S.aureus and E.coli in TSB and PW broth of LTAAg-1_100%.

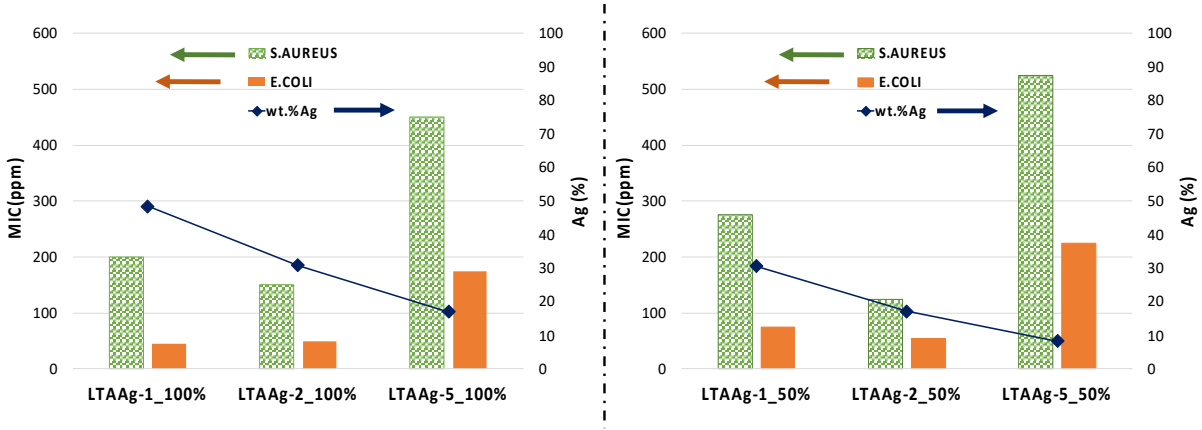

Figure 5: Bactericidal activity (MIC) against S.aureus and E.coli in TSB with total and half silver exchange LTA zeolites.

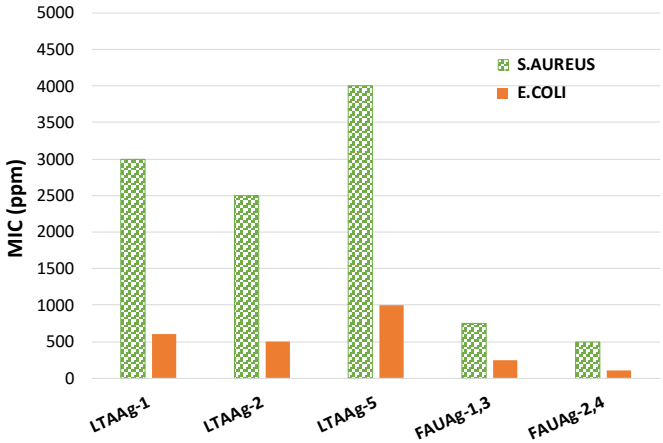

Figure 6: Bactericidal activity (MIC) against S.aureus and E.coli in TSB with different zeolites with 2 wt.% Ag.

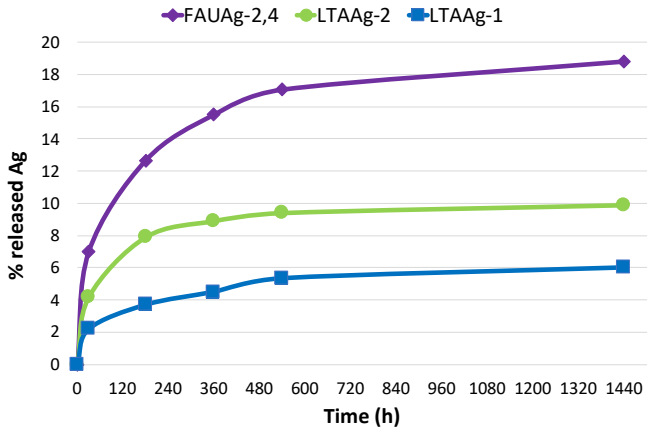

Figure 7: Ag lixiviation studies of three different zeolites at PW

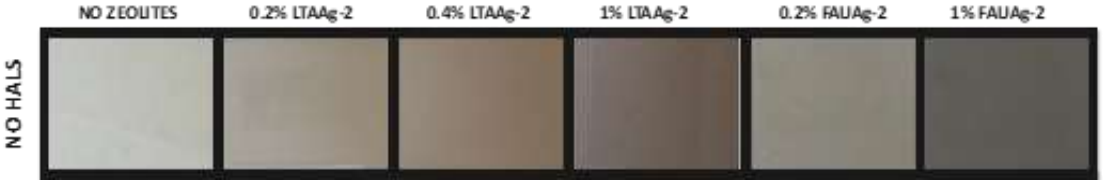

Figure 8: Images of the polymeric plates prepared with different % and diverse Ag-zeolites

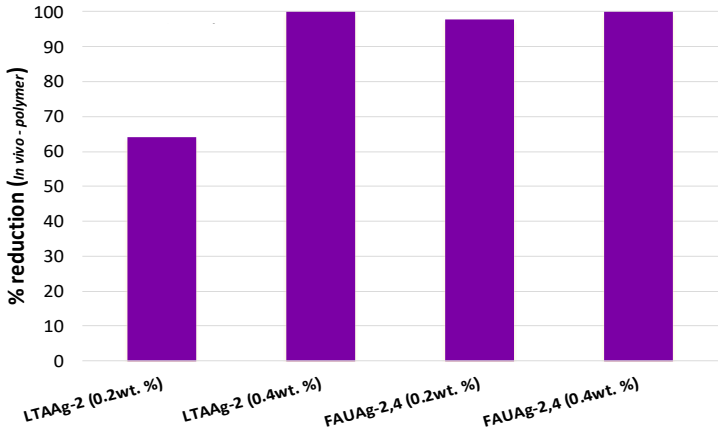

Figure 9: Biocidal properties of the surface of polymeric plates functionalized by different amount of LTAAg-2 and FAUAg-2.4, following JIS Z 2108:2010

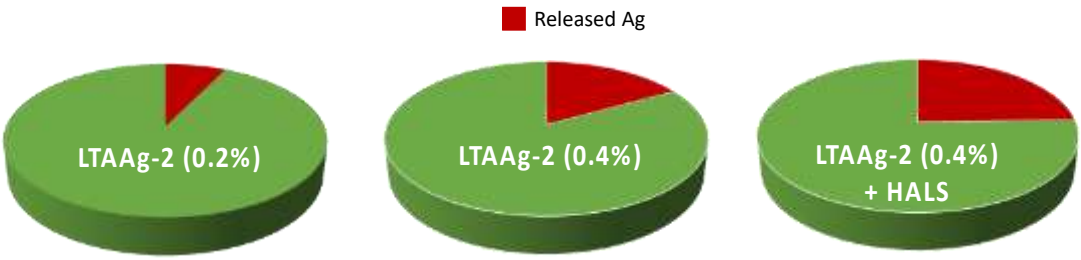

Figure 10: Percentage of released Ag from different polymeric plates